Chapter 4

Temperature and pH-Responsive "Smart" Carbon Nanotube Dispersions

Dan Wang and Liwei Chen

Abstract

Carbon nanotubes (CNTs) are a family of all-carbon quasi one-dimensional nanomaterials that are highly hydrophobic and typically aggregated in bundles. Recent accomplishments in dispersing CNTs in aqueous solutions open possibilities for their new applications in biomedicine. In many occasions, biological and biomedical applications demand an actuation mechanism; thus, it is highly desirable to control the dispersion and aggregation of CNTs in aqueous solutions with external stimuli. Here, we report two "smart" single-walled CNT (SWNT) aqueous dispersions that respond to temperature and pH changes through environment-responsive polymers, poly (*N*-isopropylacrylamide) (PNIPAAm) and Poly-L-lysine (PLL).

Key words: Single-walled carbon nanotube, Dispersion, Aggregation, Temperature-responsive, pH-responsive, poly (*N*-isopropylacrylamide), Poly-L-lysine, Atomic force microscopy, Fluorescence

1. Introduction

The unique all carbon quasi one-dimensional structure of SWNTs has intrigued much fundamental research on their mechanical, thermal, and electrical properties as well as potential applications in nanocomposites, field emission displays, and molecular electronics (1–5). Recent introduction of individually dispersed SWNTs to aqueous and biology compatible media has opened new frontiers of carbon nanotubes in biology and nanomedicine (6–8). Generally speaking, the surface of as-produced SWNTs is highly hydrophobic; and thus SWNTs exist in aggregated bundles. SWNT dispersions in organic or aqueous solvents can be obtained by either covalent functionalization or non-covalent solublization, with the latter being more favored for the preservation of nanotube structure and properties. Since non-covalent

K. Balasubramanian and M. Burghard (eds.), *Carbon Nanotubes: Methods and Protocols*, Methods in Molecular Biology, vol. 625,
DOI 10.1007/978-1-60761-579-8_4,

interactions with SWNT sidewalls (π–π stacking, van-der-Waals interactions, and hydrophobic interactions) do not require specificity and directionality, a surprisingly large variety of small molecule surfactants and water-soluble amphiphilic polymers are suitable for this purpose (9–17). Multi-functional polymer surfactants are also exploited for the separation (14, 16–18), alignment (19, 20), and hierarchical assembly of SWNTs (21), as well as for attaching fluorescent chromophore and biologically active cargos to SWNTs (22, 23).

Many biomedical applications involve active processes, for example, drug and/or gene delivery involves active release of load at target locations; photothermal and photodynamic therapies involve light-induced actuation: heating and photochemistry, respectively. Utilization of amphiphilic polymer surfactants in SWNT dispersion enables potential actuation mechanisms via selected multi-functional polymers (24). Here, we discuss two "smart" SWNT dispersions that respond to temperature and pH changes using poly (*N*-isopropylacrylamide) (PNIPAAm) and poly-L-lysine (PLL). The action in response to temperature or pH stimuli is the aggregation of SWNTs in the dispersion. Controlled aggregation of SWNT may help clogging local blood vessel, "deliver" SWNT along with attached load by precipitating from circulation, or enhance photothermal effects. Therefore, the two environmentally responsive SWNT dispersions presented here are pioneering examples of SWNT actuation in biocompatible environments, and they may lead to more sophisticated biotechnologies in the future.

PNIPAAm has long been known as a temperature responsive polymer (25). The structure of PNIPAAm contains balanced hydrophilicity from amide bonds and hydrophobicity from hydrocarbon main chain and isopropyl groups on side chains. At temperatures lower than the lower critical solution temperature (LCST, ~33°C for PNIPAAm), PNIPAAm assumes an extended chain conformation in which N and O atoms in amid bonds form H-bonding with surrounding water molecules. When the temperature is higher than the LCST, water molecules are released to maximize entropy while amid groups form intra-chain H-bonding among themselves; thus, the polymer chain takes a coiled and compact conformation (26–28). The extended conformation of PNIPAAm at low temperature allows the amphiphilic polymer chain to cover a large area of SWNT surface in dispersion. Raising temperature causes the chain conformation to shrink and thus exposes hydrophobic SWNT surface to water. This provides a driving force for SWNTs, which are dispersed at low temperatures, to aggregate into small bundles.

PLL is an amphiphilic polyelectrolyte that contains both hydrophobic hydrocarbon moieties and partially protonated primary amine groups. SWNTs interact with PLL in aqueous

environment because of two interactions: one is hydrophobic interaction between PLL hydrocarbon linker moieties ($-C_4H_8-$) and SWNT sidewalls; the other is cation-π interaction between protonated amine groups and the π-electron system of SWNTs (26). The cation-π interaction is completely turned off at pH value equal to or higher than the isoelectric point of lysine (9.7) due to the deprotonation of $-NH_3^+$ groups. The hydrophobic interaction between $-C_4H_8-$ linker and SWNT is also affected by pH via changes in the secondary structure of PLL. PLL chain adopts the α-helix conformation at high pH but changes to uncoiled conformations in acidic or neutral pH due to the electrostatic repulsion among side chain cations (29, 30). Since both interaction mechanisms between PLL and SWNT respond to the pH change of the solution, the PLL–SWNT dispersion is expected and indeed observed to be pH sensitive.

2. Materials

1. HiPCO SWNT powders, purified grade (Carbon Nanotechnologies, Inc., Houston, TX).
2. Poly (*N*-isopropylacrylamide), molecular weight 20,000–25,000 (Aldrich).
3. 0.1 % (w/v) Poly-L-lysine solution in H_2O (Sigma).
4. Sonicator VCX 130 (Sonix, Newtown, CT).
5. Atomic force microscopy (AFM) microscope MFP3D (Asylum Research, Santa Barbara, CA).
6. AFM probes NSC15/AlBS (MikroMasch USA, Wilsonville, OR) with resonance frequency around 325 KHz.
7. Fluorescence NS1 NanoSpectralyzer (Applied NanoFluorescence, LLC, Houston, TX).
8. Spectropolarimeter Jasco-715 (Jasco Inc., Easton, MD).

3. Methods

3.1. SWNT Dispersion in PNIPAAm

3.1.1. Preparation of PNIPAAm–SWNT Dispersion

1. 10 mg/ml of PNIPAAm solution is prepared by dissolving 30 mg PNIPAAm in 2.4 ml water and then adding 0.6 ml of 0.1 M NaOH solution (see Note 1).
2. Add ~1 mg of HiPCO SWNT powder to 3 ml of 10 mg/ml PNIPAAm solution. This mixture is sonicated for 90 min in an ice-water bath at a power level of 130 W (Fig. 1).

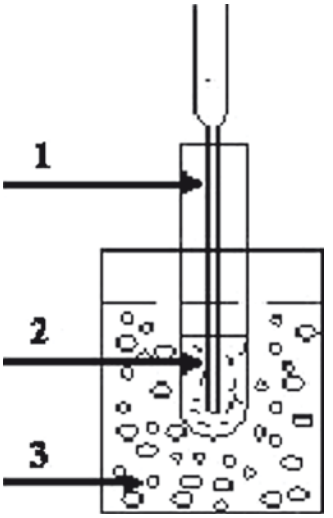

Fig. 1. Experimental setup for SWNT sonication: (1) sonication probe; (2) polymer and SWNTs; (3) ice-water bath

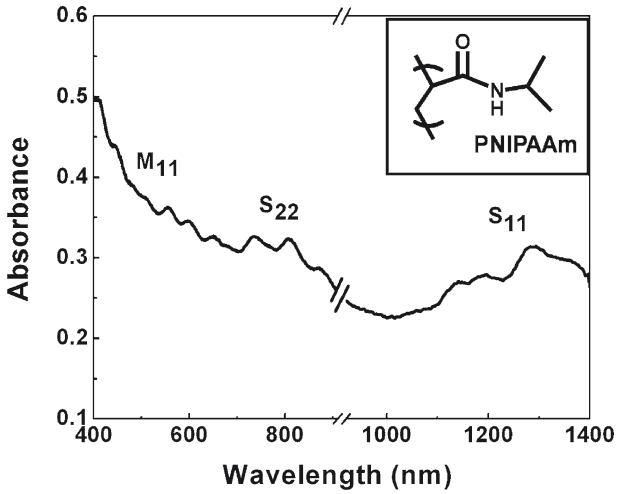

Fig. 2. Absorption spectrum of PNIPAAm–SWNT dispersion. *Inset:* the structure of PNIPAAm

3. The solution is centrifuged for 5 min at 800 × *g* and 3 min at 2,300 × *g* to yield a PNIPAAm–SWNT dispersion in the supernatant (see Note 2).

3.1.2. Spectroscopic Characterization of PNIPAAm–SWNT Dispersion

The absorption spectrum (Fig. 2) showed resolved peaks in spectral ranges for the first interband transitions for metallic SWNTs (M_{11}), the first (S_{11}) and second (S_{22}) interband transitions for semiconducting SWNTs (31, 32). The Raman spectrum (Fig. 3) showed features of SWNTs including the radial breathing mode (RBM), the tangential G-band, the disorder induced D-band,

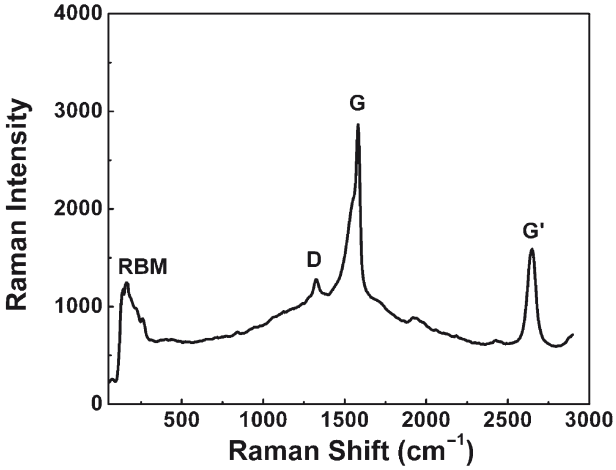

Fig. 3. Raman spectrum of PNIPAAm–SWNT dispersion

and its second-order harmonic, the G′-band (33). The van Hove peaks in absorption spectrum and the low intensity of D-band in Raman spectrum indicate that PNIPAAm molecules are non-covalently physisorbed on the sidewall of SWNTs (26).

3.1.3. Temperature Response of PNIPAAm–SWNT Complexes

To test the temperature response of the SWNT dispersion in PNIPAAm, we use atomic force microscopy to characterize the morphology of individual PNIPAAm–SWNT complexes and fluorescence spectra to characterize the response at the ensemble level. The PNIPAAm–SWNT complexes were first measured at room temperature, then heated in a 40°C water bath for 2 min and measured after cooling to room temperature, finally re-dispersed by 2 min sonication at 0°C and measured at room temperature. Photographs (Fig. 4) showed the solution becomes turbid after heating due to the aggregation of free PNIPAAm. When the solution is cooled down to room temperature, it became clear again.

1. AFM sample preparation: 10 µl of 0.1% w/v PLL solution was spin-coated onto a freshly cleaved mica and then 10 µl of the PNIPAAm–SWNT dispersion was spin coated on this substrate. The samples were then rinsed with deionized water and dried with argon gas. All AFM images were taken at room temperature and ambient conditions in AC mode. The images show that SWNTs aggregate into larger bundles (4–20 nm diameter) after heating (Fig. 5) (see Note 3). However, after 2 min sonication in 0°C ice-water bath, SWNTs are re-dispersed individually or in small bundles similar to those from the original dispersion (<5 nm) (Fig. 5).
2. Fluorescence spectra are taken at room temperature using an excitation wavelength of 785 nm. At this excitation energy, semiconducting SWNTs with different diameters fluoresce at their respective S_{11} band transition energies and form a

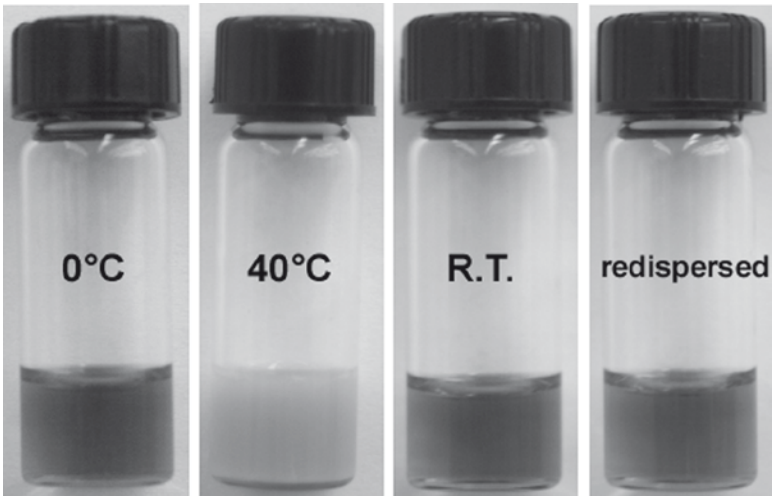

Fig. 4. Photographs of PNIPAAm–SWNT dispersions, from *left* to *right*: PNIPAAm–SWNT dispersions at 0°C, 40°C, cooled to room temperature, and redispersed by 2 min sonication at 0°C

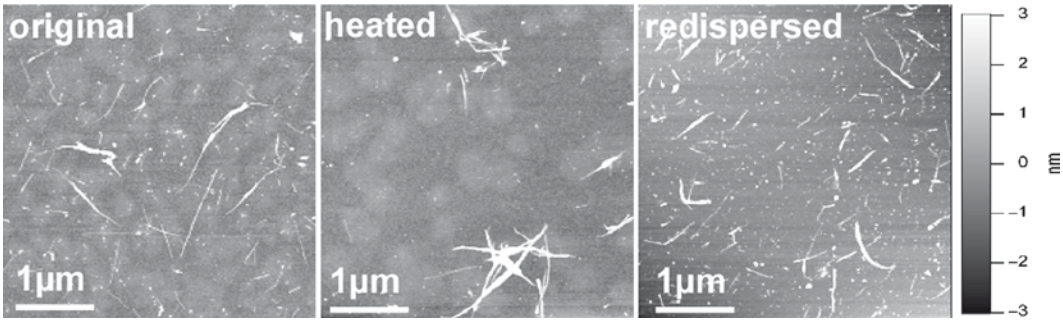

Fig. 5. AFM images of PNIPAAm–SWNT complexes, from *left* to *right*: original dispersion, heated at 40°C for 2 min, redispersed by sonicating at 0°C for 2 min

spectrum with multiple peaks. Aggregation of SWNTs results in quenching of the fluorescence. Partial quenching of nanotube fluorescence after heating suggests bundling of SWNTs in the dispersion and the bundling effect is uniform across SWNTs with all different diameters (Fig. 6). The fluorescence intensity recovers to the level of the original dispersion after re-dispersion (Fig. 6), which indicates that the temperature stimulated switching is reversible (see Note 4).

3.2. SWNT Dispersion in PLL

3.2.1. Preparation and Spectroscopic Characterization of PLL–SWNT Dispersion

1. Add ~1 mg of purified HiPCO SWNT powders to 2 ml of 0.1% w/v Poly-L-lysine solution and sonicate for an hour in ice-water bath at a power level of 130 W.
2. Centrifuge the mixture for 10 min at 9,400 × *g* to yield the PLL–SWNT complexes in the supernatant. The pH of as-prepared PLL–SWNT complexes solution is about 7.0.

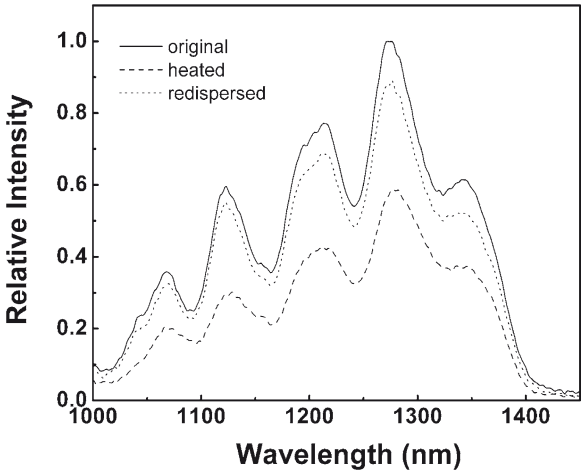

Fig. 6. Fluorescence spectra of PNIPAAm–SWNT dispersions before (*solid trace*) and after (*dash trace*) heating in 40°C, and after redispersion 2 min sonication at 0°C (*dot trace*) (Excited at 785 nm)

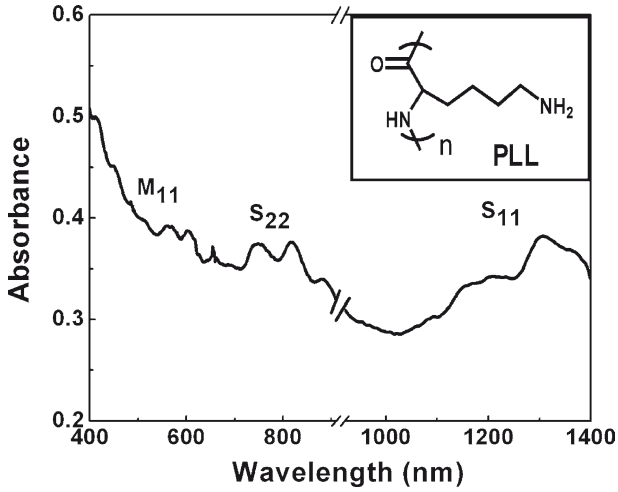

Fig. 7. Absorption spectrum of PLL–SWNT dispersion. *Inset:* the structure of PLL

3. Take absorption (Fig. 7) and Raman spectra (Fig. 8) of PLL–SWNT dispersion.

3.2.2. pH Response of PLL–SWNT Complexes

Atomic force microscopy and fluorescence spectra are used to characterize the pH response of the SWNT dispersion in PLL solution. Circular dichroism (CD) spectroscopy is used to verify secondary structure changes of PLL at different pH values.

1. The pH of the PLL–SWNT solution was adjusted from 7.0 to 4.1, then increased to 9.7, decreased back to 8.3, and finally

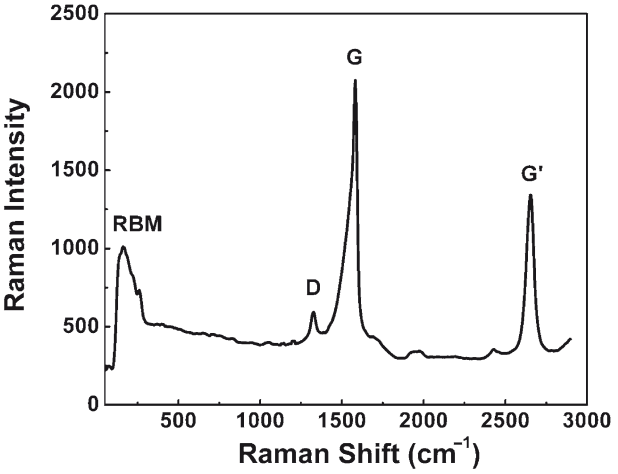

Fig. 8. Raman spectrum of PLL–SWNT dispersion

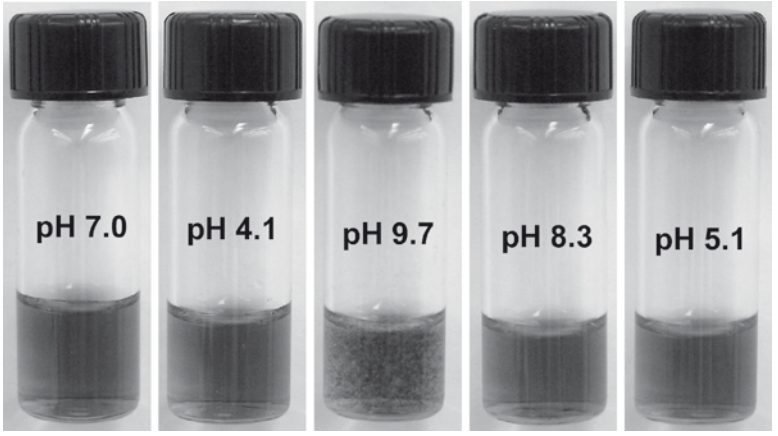

Fig. 9. Photographs of PLL–SWNT dispersions at different pH values

decreased to 5.1 by adding 1.5 M HCl or NaOH solutions. Each change of pH is followed by 10 min sonication in ice-water bath. The photographs (Fig. 9) show that the solution becomes cloudy at pH 9.7 due to the aggregation of SWNTs.

2. AFM samples were prepared by spin coating 10 µl of the PLL–SWNT dispersion onto a fleshly cleaved mica substrate followed by rinsing with dionized water and drying with argon gas. Imaging conditions are the same as that in PNIPAAm–SWNT measurements. AFM images (Fig. 10) show SWNTs are individually dispersed or in small bundle (<5 nm) in acidic and neutral environments but aggregate into large bundles at pH 8.3. At pH 9.7, SWNTs coalesce into big bundles, precipitate out of the solution, and could not be imaged with AFM.

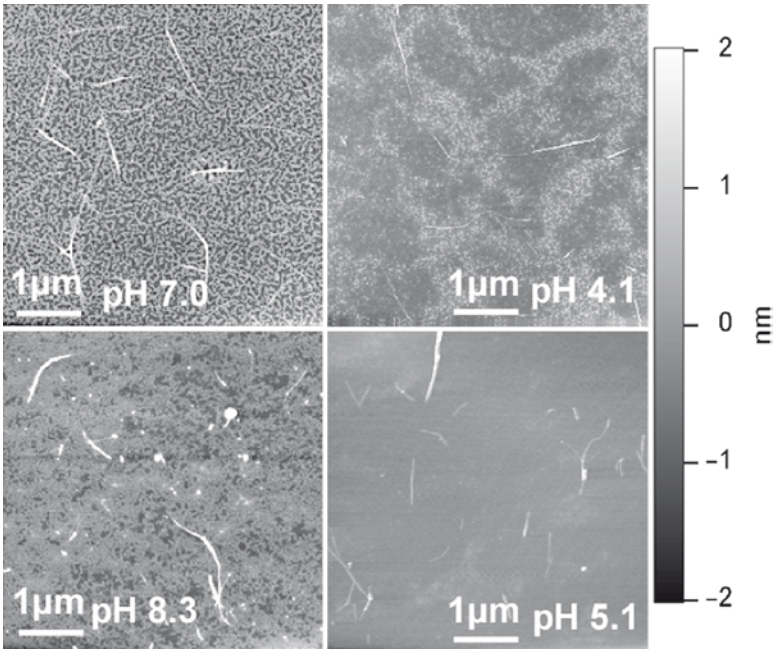

Fig. 10. AFM images of PLL–SWNT complexes at different pH values

3. Fluorescence spectra of PLL–SWNT dispersions at different pH values were taken and excited at 785 nm. Figure 11 shows that SWNT emission is partially quenched due to aggregation at pH 9.7 but remains largely unchanged in acidic and neutral environments.
4. Circular dichroism (CD) spectra of PLL–SWNT complexes were recorded at different pH values. The CD spectra of PLL–SWNT complexes in an acidic or neutral pH (Fig. 12) show a single negative peak around 200 nm, which is characteristic of uncoiled conformation. At pH 9.7, the spectrum displays two negative bands in the 200–230 nm range, characteristic of the α-helix conformation (29, 34).

4. Notes

1. All solutions are prepared in deionized water (18.2 MΩ cm, Millipore).
2. The PNIPAAm–SWNT dispersion is stable at room temperature for weeks with little or no precipitation, but it can not withstand high speed centrifugation.
3. Sonicating the dispersion while it is heated at 40°C does not prevent the complexes from aggregating.

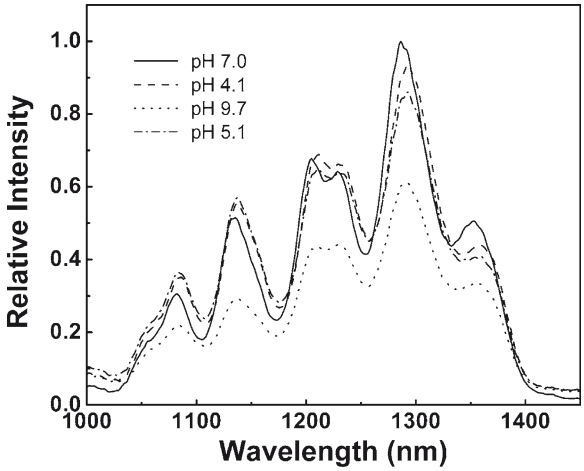

Fig. 11. Fluorescence spectra of PLL–SWNT dispersions at different pH values excited at 785 nm

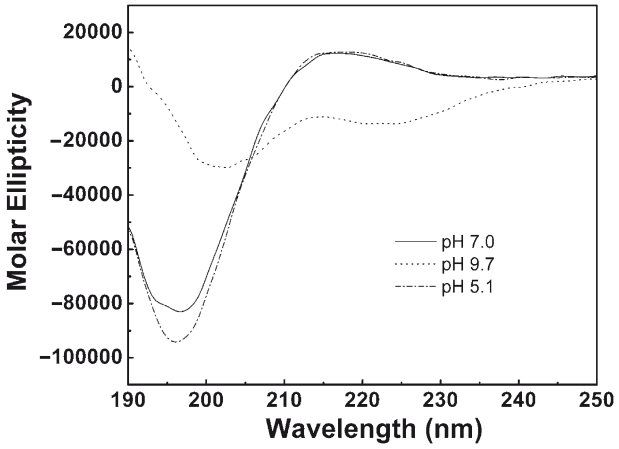

Fig. 12. Circular dichroism spectra of PLL–SWNT complexes at different pH values

4. Spectrum at 40°C could not be obtained because of the strong scattering of aggregated free PNIPAAm and PNIPAAm–SWNT complexes. We measure the fluorescence spectra when the solution cools down to room temperature.

Acknowledgments

This work is partially supported by the Nanobiotechnology Initiative at Ohio University. D. W. thanks Ohio University Condensed Matter and Surface Sciences program for partial support.

References

1. Kim SN, Rusling JF, Papadimitrakopoulos F (2007) Carbon nanotubes for electronic and electrochemical detection of biomolecules. Adv Mater 19:3214–3228
2. Avouris P, Chen Z, Perebeinos V (2007) Carbon-based electronics. Nat Nanotechnol 2:605–615
3. Snow ES, Perkins FK, Robinson JA (2006) Chemical vapor detection using single-walled carbon nanotubes. Chem Soc Rev 35:790–798
4. Lu W, Lieber CM (2007) Nanoelectronics from the bottom up. Nat Mater 6:841–850
5. Prato M, Kostarelos K, Bianco A (2008) Functionalized carbon nanotubes in drug design and discovery. Acc Chem Res 41:60–68
6. Chen X, Tam UC, Czlapinski JL, Lee GS, Rabuka D, Zettl A, Bertozzi CR (2006) Interfacing carbon nanotubes with living cells. J Am Chem Soc 128:6292–6293
7. Cherukuri P, Gannon CJ, Leeuw TK, Schmidt HK, Smalley RE, Curley SA, Weisman RB (2006) Mammalian pharmacokinetics of carbon nanotubes using intrinsic near-infrared fluorescence. Proc Natl Acad Sci USA 103:18882–18886
8. Lacerda L, Bianco A, Prato M, Kostarelos K (2006) Carbon nanotubes as nanomedicines: from toxicology to pharmacology. Adv Drug Deliv Rev 58:1460–1470
9. Chatterjee T, Yurekli K, Hadjiev VG, Krishnamoorti R (2005) Single-walled carbon nanotube dispersions in poly(ethylene oxide). Adv Funct Mater 15:1832–1838
10. Dieckmann GR, Dalton AB, Johnson PA, Razal J, Chen J, Giordano GM, Munoz E, Musselman IH, Baughman RH, Draper RK (2003) Controlled assembly of carbon nanotubes by designed amphiphilic peptide helices. J Am Chem Soc 125:1770–1777
11. Karajanagi SS, Yang HC, Asuri P, Sellitto E, Dordick JS, Kane RS (2006) Protein-assisted solubilization of single-walled carbon nanotubes. Langmuir 22:1392–1395
12. Moore VC, Strano MS, Haroz EH, Hauge RH, Smalley RE, Schmidt J, Talmon Y (2003) Individually suspended single-walled carbon nanotubes in various surfactants. Nano Lett 3:1379–1382
13. Numata M, Asai M, Kaneko K, Bae AH, Hasegawa T, Sakurai K, Shinkai S (2005) Inclusion of cut and as-grown single-walled carbon nanotubes in the helical superstructure of schizophyllan and curdlan (ss-1, 3-glucans). J Am Chem Soc 127:5875–5884
14. Ortiz-Acevedo A, Xie H, Zorbas V, Sampson WM, Dalton AB, Baughman RH, Draper RK, Musselman IH, Dieckmann GR (2005) Diameter-selective solubilization of single-walled carbon nanotubes by reversible cyclic peptides. J Am Chem Soc 127:9512–9517
15. Wang D, Ji WX, Li ZC, Chen LW (2006) A biomimetic "polysoap" for single-walled carbon nanotube dispersion. J Am Chem Soc 128:6556–6557
16. Zheng M, Jagota A, Semke ED, Diner BA, McLean RS, Lustig SR, Richardson RE, Tassi NG (2003) DNA-assisted dispersion and separation of carbon nanotubes. Nat Mater 2:338–342
17. Zheng M, Jagota A, Strano MS, Santos AP, Barone P, Chou SG, Diner BA, Dresselhaus MS, McLean RS, Onoa GB, Samsonidze GG, Semke ED, Usrey M, Walls DJ (2003) Structure-based carbon nanotube sorting by sequence-dependent DNA assembly. Science 302:1545–1548
18. Huang X, McLean RS, Zheng M (2005) High-resolution length sorting and purification of DNA-wrapped carbon nanotubes by size-exclusion chromatography. Anal Chem 77:6225–6228
19. McLean RS, Huang X, Khripin C, Jagota A, Zheng M (2006) Controlled two-dimensional pattern of spontaneously aligned carbon nanotubes. Nano Lett 6:55–60
20. Shim BS, Kotov NA (2005) Single-walled carbon nanotube combing during layer-by-layer assembly: from random adsorption to aligned composites. Langmuir 21:9381–9385
21. Wang D, Li Z-C, Chen L (2006) Templated synthesis of single-walled carbon nanotube and metal nanoparticle assemblies in solution. J Am Chem Soc 128:15078–15079
22. Kam NWS, O'Connell M, Wisdom JA, Dai H (2005) Carbon nanotubes as multifunctional biological transporters and near-infrared agents for selective cancer cell destruction. Proc Natl Acad Sci USA 102:11600–11605
23. Kam NWS, Liu Z, Dai H (2006) Carbon nanotubes as intracellular transporters for proteins and DNA: an investigation of the uptake mechanism and pathway. Angew Chem Int Ed Engl 45:577–581
24. Barone PW, Strano MS (2006) Reversible control of carbon nanotube aggregation for a glucose affinity sensor. Angew Chem Int Ed Engl 45:8138–8141

25. Schild HG (1992) Poly(N-isopropylacrylamide): experiment, theory and application. Prog Polym Sci 17:163–249
26. Wang D, Chen L (2007) Temperature and pH-responsive single-walled carbon nanotube dispersions. Nano Lett 7:1480–1484
27. Sun T, Wang G, Feng L, Liu B, Ma Y, Jiang L, Zhu D (2004) Reversible switching between superhydrophilicity and superhydrophobicity. Angew Chem Int Ed 43:357–360
28. Lin S-Y, Chen K-S, Run-Chu L (1999) Thermal micro ATR/FT-IR spectroscopic system for quantitative study of the molecular structure of poly(N-isopropylacrylamide) in water. Polymer 40:2619–2624
29. Wang Y, Chang YC (2003) Synthesis and conformational transition of surface-tethered polypeptide: poly(L-lysine). Macromolecules 36:6511–6518
30. Davidson B, Fasman GD (1967) Conformational transitions of uncharged poly-L-lysine. a Helix-random coil-b-structure. Biochemistry 6:1616–1629
31. Strano MS, Dyke CA, Usrey ML, Barone PW, Allen MJ, Shan H, Kittrell C, Hauge RH, Tour JM, Smalley RE (2003) Electronic structure control of single-walled carbon nanotube functionalization. Science 301:1519–1522
32. O'Connell MJ, Bachilo SM, Huffman CB, Moore VC, Strano MS, Haroz EH, Rialon KL, Boul PJ, Noon WH, Kittrell C, Ma J, Hauge RH, Weisman RB, Smalley RE (2002) Band gap fluorescence from individual single-walled carbon nanotubes. Science 297:593–596
33. Dresselhaus MS, Dresselhaus G, Jorio A, Souza Filho AG, Saito R (2002) Raman spectroscopy on isolated single wall carbon nanotubes. Carbon 40:2043–2061
34. Greenfield NJ, Fasman GD (1969) Computed circular dichroism spectra for the evaluation of protein conformation. Biochemistry 8:4108–4116